

Effects of acoustic waves on stick–slip in granular media and implications for earthquakes

Paul A. Johnson¹, Heather Savage^{2,3}, Matt Knuth^{2,4}, Joan Gomberg⁵ & Chris Marone²

It remains unknown how the small strains induced by seismic waves can trigger earthquakes at large distances, in some cases thousands of kilometres from the triggering earthquake, with failure often occurring long after the waves have passed^{1–6}. Earthquake nucleation is usually observed to take place at depths of 10–20 km, and so static overburden should be large enough to inhibit triggering by seismic-wave stress perturbations. To understand the physics of dynamic triggering better, as well as the influence of dynamic stressing on earthquake recurrence, we have conducted laboratory studies of stick–slip in granular media with and without applied acoustic vibration. Glass beads were used to simulate granular fault zone material, sheared under constant normal stress, and subject to transient or continuous perturbation by acoustic waves. Here we show that small-magnitude failure events, corresponding to triggered aftershocks, occur when applied sound-wave amplitudes exceed several microstrain. These events are frequently delayed or occur as part of a cascade of small events. Vibrations also cause large slip events to be disrupted in time relative to those without wave perturbation. The effects are observed for many large-event cycles after vibrations cease, indicating a strain memory in the granular material. Dynamic stressing of tectonic faults may play a similar role in determining the complexity of earthquake recurrence.

Laboratory studies of granular friction have emerged as a powerful tool for investigating tectonic fault zone processes and earthquake phenomena, including post-seismic slip, interseismic frictional restrengthening and earthquake nucleation^{7,8}. Here we explore experimentally the effects of dynamic loading on stick–slip behaviour and discuss how our results may affect understanding of earthquake processes—in particular dynamic earthquake triggering and stick–slip recurrence. Dynamic earthquake triggering involves seismic waves from one earthquake promoting or inhibiting failure on the faults they disturb. Dynamic triggering has been clearly documented in a few cases far from an earthquake source, at distances much greater than the fault radius of the triggering source^{1–4,6} (outside the traditional ‘aftershock zone’), and increasing evidence suggests that it commonly occurs near the earthquake source^{5,9}.

Experiments on sheared layers of glass beads (like those shown in Fig. 1, and described in the Methods section) exhibit stick–slip that varies with shear displacement rate, confining stress, relative humidity, granular media thickness, and particle characteristics^{10–12}; however, for fixed experimental conditions stick–slip characteristics are remarkably constant (Fig. 2). Stick–slip events are characterized by sudden, periodic shear stress drops that range from 10–30% of the maximum frictional strength. Leading up to steady-state strength, which takes several tens of seconds and shear strains of ~ 0.4 – 0.5 , we observe a material dilation and nonlinear shear-stress increase

accompanied by intermittent failure. During steady-state frictional behaviour, major stick–slip events recur very regularly but include rare, small events (for example, at 1,375 s in Fig. 2b). Each major stick–slip event is followed by elastic and then inelastic stress build-up and layer dilation. The dilation is manifested by increasing layer thickness (Fig. 2b). Layers dilate to a point of instability at which catastrophic dynamic failure and compaction occur (Fig. 2b).

The top curve of Fig. 3a shows results from an experiment identical to that of Fig. 2 except that we applied acoustic waves during shearing, commencing a few seconds before expected stick–slip failure, and continuing until the major failure event. The lower curve of Fig. 3a shows the rectified peak strain amplitude measured by the accelerometer attached to the sample (Fig. 1), along with three

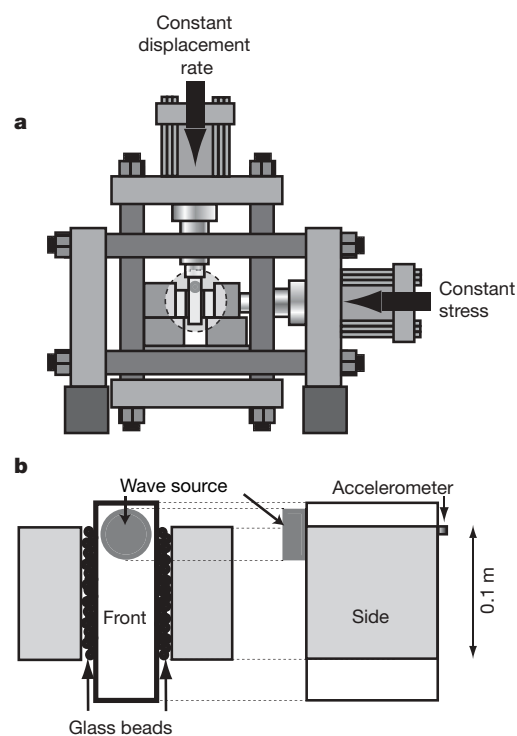


Figure 1 | Experimental apparatus. **a**, Apparatus, showing horizontal piston applying constant normal stress, and vertical piston applying a constant (vertical) displacement rate, which drives shear. The dashed circle shows the sample assembly. **b**, Sample assembly showing three-block arrangement of the double-direct shear configuration (front and side views). We note the location of the acoustic wave source and accelerometer in relation to the glass bead layers and normal stress (horizontal).

¹Geophysics Group EES-11, Los Alamos National Laboratory of the University of California, MS D443, Los Alamos, New Mexico 87545, USA. ²Department of Geosciences, Pennsylvania State University, University Park, Pennsylvania 16802, USA. ³Department of Earth and Planetary Science, University of California, Santa Cruz, California 95064, USA. ⁴Department of Geology and Geophysics, University of Wisconsin, Madison, Wisconsin 53706, USA. ⁵US Geological Survey, University of Washington, Department of Earth and Space Sciences, Box 351310, Seattle, Washington 98195-1310, USA.

intervals for which dynamic waves were applied and signals from acoustic emission from both small and large stick-slip failures.

Vibration perturbs the recurrence period of inelastic stress increase before the failure of major events and induces small-amplitude stick-slip events. In many cases one or more small stick-slip events occur during vibration, as well as cascades of delayed, small-amplitude stick-slip events (Fig. 3a, grey shading). In all cases, application of acoustic waves—even for brief intervals—has a lasting effect, such that successive major stick-slip events exhibit a strain memory of applied vibration manifest by delayed failure, disruption of recurrence interval and extended aseismic creep, despite the violent mechanical re-set that occurs during major stick-slip events (Fig. 3). We find that post-vibration, the regular recurrence does not recover.

We also apply acoustic pulses, rather than the longer-duration waves described above. Pulses are more analogous to a single seismic wave in Earth, whereas vibration may be more analogous to the near-source region where quasi-continuous-wave energy may exist for significant periods of time in the form of aftershocks. Our data show that continuous and pulse modes of dynamic triggering yield similar behaviour. See Supplementary Fig. 1, where we show a typical sequence of stick-slip events in the presence of acoustic pulses.

When we apply vibration or pulsed sound at stresses below $\sim 95\%$ of the failure strength there is little or no effect on stick-slip. This implies that the system must be in a critical state to be susceptible to dynamic triggering, which is consistent with seismic data on earthquake triggering¹³ and recent modelling¹⁴. Qualitatively, wave strain amplitudes must exceed approximately 10^{-6} for the above effects to

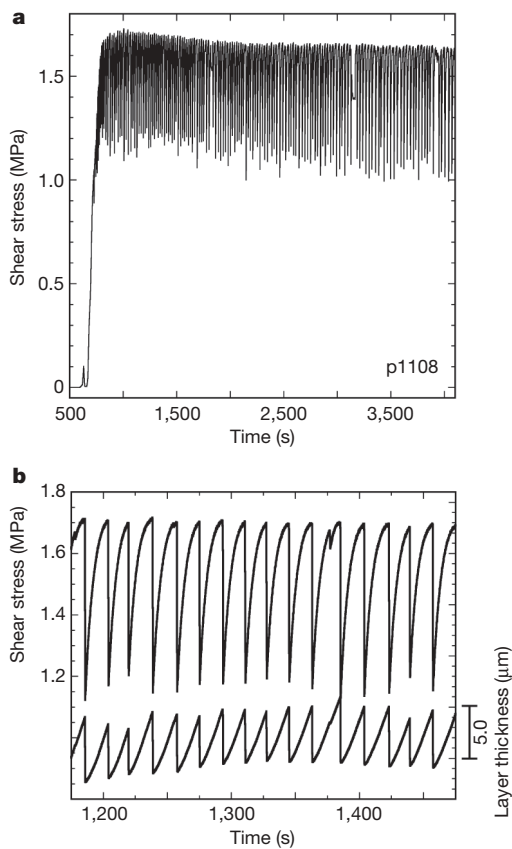


Figure 2 | Stick-slip behaviour under constant shearing rate, without vibration. **a**, Shear stress versus experiment time for a typical run. Note that maximum stick-slip stress drops are $\sim 30\%$ of the shear strength. Over the total duration of the experiment, there is a small but progressive compaction of about 1% of the glass bead layer thickness (not shown). **b**, Detail of the stick-slip cycles (top) and change in layer thickness (bottom). The layer thickness has had the overall trend removed. We note consistent failure strength, recurrence interval, and creep before stick-slip. p1108 refers to experiment number.

58

be observed (Supplementary Fig. 2), consistent with dynamic triggering observations for real earthquakes¹⁵. When the system is driven with vibration amplitudes corresponding to strains $< 10^{-6}$ there is no obvious effect on stick-slip; however, we emphasize that this should be further quantified in future experiments.

Analysis of the primary stick-slip recurrence intervals for otherwise identical experiments with and without vibration shows that failure becomes progressively more erratic and, on average, lengthens with time in experiments with wave excitation (Fig. 4a). Repeated experiments with both vibration and pulse-mode verify that this effect is real. We find that the scatter relative to the mean increases with accumulated time in experiments with vibration. Also, although the primary stick-slip recurrence interval increases significantly due to acoustic waves, the stress-drop magnitude and variation increase only slightly (Fig. 4b).

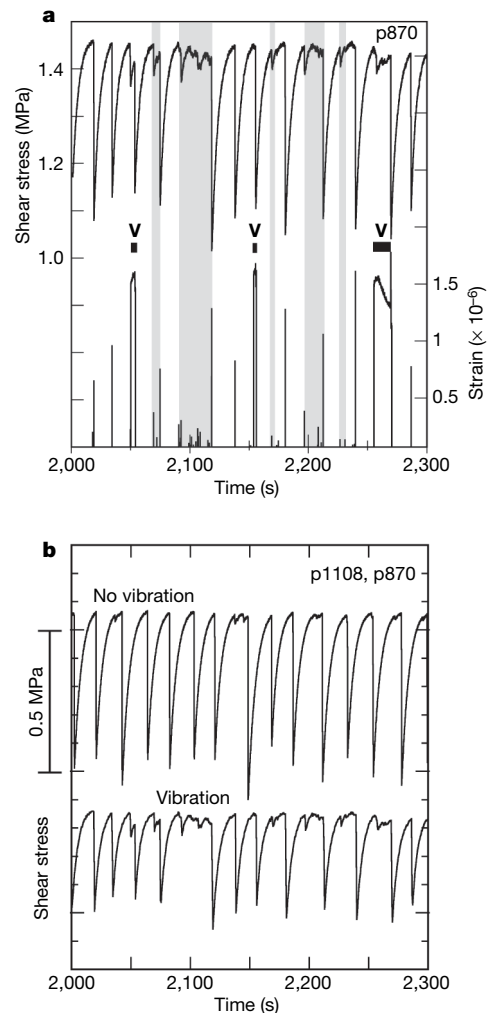


Figure 3 | Stick-slip with and without vibration. **a**, Stick-slip behaviour under constant shearing rate, with vibration. Shear stress versus experiment time (upper curve); and measured, rectified strain amplitudes of the detected acoustic waves (lower curve). The letter 'V' denotes times and thick black horizontal bars indicate the durations of vibration. Vibration has a marked influence on the stick-slip behaviour. For instance, the applied vibration at $\sim 2,050$ s produces an immediate, small-magnitude stick-slip. The two successive major stick-slips that follow exhibit longer recurrence times as well as multiple small stick-slip events in between—these are triggered events. Regions of triggered events are shaded light grey. Similarly, irregular cycles occur following the applied vibration at 2,155 s. Vibration applied at $\sim 2,255$ s produces an immediate small-magnitude stick-slip event and an increased major-event recurrence interval. **b**, Comparison of non-vibration versus vibration, emphasizing increased recurrence and irregular behaviour, including triggering, due to acoustic waves. p870 and p1108 refer to experiment numbers.

We have described three primary experimental observations: (1) acoustic waves disrupt recurrence intervals and, to a lesser degree, stress drops of large magnitude events; (2) acoustic waves trigger immediate and delayed small-magnitude events, some aseismic; and (3) strain memory of acoustic perturbation is maintained through successive large-magnitude stick–slips. We assess the implications of these results for dynamic earthquake triggering by considering that the primary slick–slip events represent tectonic earthquakes and that the vibration-induced events represent triggered earthquakes.

The overall trend of increasing stress drop (and maximum frictional strength) with recurrence interval is consistent with a large body of previous laboratory and field observations⁸ showing that maximum frictional strength increases linearly with the log of recurrence interval between slip events. Vibration diminishes the rate at which stress drop increases with inter-event time, notably creating greater irregularity in stick–slip recurrence interval. The commonly used class of rate-state frictional models explicitly predicts that the rate of strengthening is proportional to the product of the normal stress and the frictional constitutive parameters⁸. Because we hold the normal stress constant, this implies that vibration alters frictional properties, despite the fact that perturbation amplitudes ($\sim 10^4$ Pa) are less than 1% of the normal load. We suggest that the irregularity in recurrence that we observe in our experiments mimics that observed for tectonic faults in the Earth's crust, and reflects a complex process of disrupting the internal fault zone structure.

We find that vibration has measurable effects only when the system is in a critical state, approaching failure (for example, see Fig. 3a).

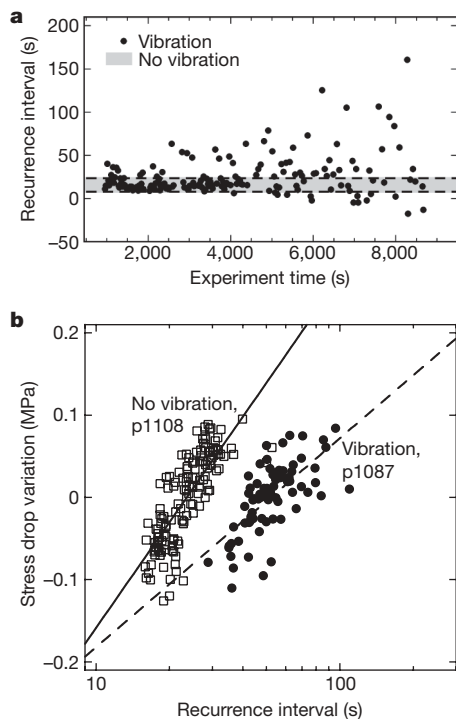


Figure 4 | Stick-slip recurrence time and stress drop comparing vibration and non-vibration experiments. **a**, Recurrence versus experiment time for runs with vibration (solid circles) and without. The shaded region and dashed lines show the mean recurrence interval of ± 1 standard deviation. Data trend removed. Compared to the non-vibration experiments, both the scatter and average recurrence interval increases progressively in experiments with vibration. **b**, Stress-drop variation versus recurrence for experiments conducted with and without vibration. We cannot compare stress-drop amplitudes directly owing to minor differences from one experiment to the next; however, when we compare the variation of stress drop to the experimental mean, we see a clear trend of longer recurrence interval for a given change in stress drop.

Application of acoustic waves also has a measurable effect only for experiments conducted at relatively small normal stresses, approximately 4–5 MPa. We have explored higher horizontal loads (up to ~ 18 MPa) for which we did not see a vibrational effect; perhaps the vibration amplitude was not sufficiently large to produce an effect. Nevertheless, the laboratory experiments do imply that dynamic earthquake triggering at seismic strain amplitudes is most efficient at low effective stress (normal load minus pore pressure) for faults in a critical state. Some field-based studies also point to a connection between earthquake triggering and low effective stress and/or faults near failure^{6,16,17}, although this is a point of some debate¹⁸.

One mystery regarding dynamic earthquake triggering is that it can take place minutes, hours or days after the seismic perturbation. Our experiments show delayed failures following acoustic perturbations, frequently manifesting as cascades of small events. We do not yet understand the physics responsible for this observation; however, we speculate that triggered events, as well as the recurrence and stress-drop disruptions are manifestations of frictional contact mechanics coupled with granular processes. Previous work shows that stick–slip initiates as failure of a contact junction between beads in highly stressed chains of particles^{11,12}. Granular memory effects are presumably the result of similar processes.

We posit that acoustic waves disrupt granular force chains, leading to material softening and simultaneous weakening (granular flow), similar to what is described in a recently proposed phenomenological model¹⁹. The manifestation of the acoustic disruption may take place immediately or later in time (strain ‘memory’). The vibration-induced memory itself may be maintained as frictional instability at a number of grain contacts that persist through one or more stick–slip cycles, and is reminiscent of dynamically induced strain memory, known as ‘slow dynamics’, observed in nonlinear dynamical experiments on glass bead packs¹⁹. The memory is also suggestive of statically induced rate-dependent effects observed in sheared granular materials, such as ‘ageing’^{7,20}. We attempted to erase vibration-induced memory by ceasing shear loading to allow the material to heal, as well as by changing normal stress to repack the grains, but neither approach succeeded.

Our previous work shows that permanent damage to the grains themselves is negligible¹² and therefore cannot be the origin of the behaviours observed. Moreover, acoustical studies in three-dimensional glass bead packs under similar wave strain amplitudes, and under (smaller) static stresses of 0.02–0.1 MPa, show no evidence for grain rearrangement; however, the material exhibits very small, irreversible compaction as well as nonlinear-induced modulus softening and slow dynamics²¹. Hertz–Mindlin contact mechanics describe these observations²¹. The compaction we measure in our experiments without vibration is small and does not lead to instability. The addition of vibration shows additional compaction but it is extremely small. Taken together, the observations suggest that minute compaction plays a part in what we observe, but there is no clear evidence suggesting that it is the cause. Our data do not rule out the possibility that instability is abetted, or initiated, by localized compaction (for example, within a shear band in the layer²²), which would be invisible to our measurements. Local compaction within a granular material would reduce normal stress at contact junctions, which could lead to stick–slip instability. For the moment, the origin of what we observe when stick–slip is combined with vibration remains unknown.

The origin of dynamic earthquake triggering by transient seismic waves is a complex problem. Our results show that granular-friction processes are consistent with two as-yet-unexplained observations in earthquake seismology: (1) small-amplitude waves can trigger both immediate failure and delayed failure relative to the strain transient, and (2) earthquake recurrence patterns are complex. Understanding the role of vibration-induced disruption of earthquake recurrence could have significant implications for seismic hazard assessment and reliable forecasting of earthquakes.

METHODS SUMMARY

In our experimental study of acoustic waves interacting with a laboratory-scale fault system, we employ a double-direct shear configuration to shear 4-mm layers of glass beads at constant normal stress (1–18 MPa), using shearing rates of $1\text{--}100\ \mu\text{m s}^{-1}$ (Fig. 1). Class IV bead dimensions are 105–149 μm in diameter. Layers are subject to either continuous vibration or wave pulses of 10–20 cycles at 1–20 kHz, with strain amplitudes ranging from $<5 \times 10^{-7}$ to 8×10^{-6} , or alternatively, to no wave excitation. An acoustic source and accelerometer are mounted directly on the central shearing block (Fig. 1b). We measure stresses, displacements and wave-induced strains continuously throughout shearing.

Full Methods and any associated references are available in the online version of the paper at www.nature.com/nature.

Received 23 July; accepted 31 October 2007.

- Hill, D. P. *et al.* Seismicity remotely triggered by the magnitude 7.3 Landers, California, earthquake. *Science* **260**, 1617–1623 (1993).
- Gomberg, J., Bodin, P., Larson, K. & Dragert, H. Earthquake nucleation by transient deformations caused by the $M = 7.9$ Denali, Alaska earthquake. *Nature* **427**, 621–624 (2004).
- Brodsky, E., Karakostas, V. & Kanamori, H. A. New observation of dynamically triggered regional seismicity: Earthquakes in Greece following the August, 1999, Izmit, Turkey earthquake. *Geophys. Res. Lett.* **27**, 2741–2744 (2000).
- Hough, S. E. Triggered earthquakes and the 1811–1812 New Madrid, Central United States earthquake sequence. *Bull. Seismol. Soc. Am.* **91**, 1574–1581 (2001).
- Gomberg, J., Bodin, P. & Reasenber, P. A. Observing earthquakes triggered in the near field by dynamic deformations. *Bull. Seismol. Soc. Am.* **93**, 118–138 (2003).
- Brodsky, E. & Prejean, S. G. New constraints on mechanisms of remotely triggered seismicity at Long Valley Caldera. *J. Geophys. Res.* **110**, 4302–4316 (2005).
- Marone, C. Laboratory-derived friction laws and their application to seismic faulting. *Ann. Rev. Earth Planet. Sci.* **26**, 643–696 (1998).
- Scholz, C. H. *The Mechanics of Earthquakes and Faulting* 2nd edn (Cambridge Univ. Press, 2002).
- Felzer, K. & Brodsky, E. Evidence for dynamic aftershock triggering from earthquake densities. *Nature* **441**, 735–738 (2006).
- Nasuno, S., Kudrolli, A., Bak, A. & Gollub, J. P. Time-resolved studies of stick-slip friction in sheared granular layers. *Phys. Rev. E* **58**, 2161–2171 (1998).
- Mair, K., Frye, K. M. & Marone, C. Influence of grain characteristics on the friction of granular shear zones. *J. Geophys. Res.* **107**, ECV4–1–9 (2002).
- Anthony, J. L. & Marone, C. Influence of particle characteristics on granular friction. *J. Geophys. Res.* **110**, B08409, doi:10.1029/2004JB003399 (2005).
- Freed, A. M. Earthquake triggering by static, dynamic, and postseismic stress transfer. *Annu. Rev. Earth Planet. Sci.* **33**, 335–367 (2005).
- Ziv, A. What controls the spatial distribution of remote aftershocks? *Bull. Seismol. Soc. Am.* **96**, 2231–2241 (2007).
- Gomberg, J. & Johnson, P. A. Dynamic triggering of earthquakes. *Nature* **473**, 830 (2005).
- Zoback, M. D. & Beroza, G. Evidence for near-frictionless faulting in the 1989 (M 6.9) Loma Prieta, California, earthquake and its aftershocks. *Geology* **21**, 181–185 (1993).
- Beeler, N. M. & Lockner, D. A. Why earthquakes correlate weakly with the solid Earth tides: effects of periodic stress on the rate and probability of earthquake occurrence. *J. Geophys. Res.* **108**, 2391–2408 (2003).
- Scholz, C. H. Evidence for a strong San Andreas fault. *Geology* **28**, 163–166 (2000).
- Johnson, P. A. & Jia, X. Nonlinear dynamics, granular media and dynamic earthquake triggering. *Nature* **473**, 871–874 (2005).
- Hartley, R. R. & Behringer, R. P. Logarithmic rate dependence of force networks in sheared granular materials. *Nature* **421**, 928–931 (2003).
- Brunet, T., Jia, X. & Johnson, P. Transitional, elastic-nonlinear behaviour in dense granular media. *Geophys. Res. Lett.* (submitted).
- Morgan, J. K. & Boettcher, M. S. Numerical simulations of granular shear zones using the distinct element method: I. Shear zone kinematics and the micromechanics of localization. *J. Geophys. Res.* **104**, 2703–2719 (1999).

Supplementary Information is linked to the online version of the paper at www.nature.com/nature.

Acknowledgements Funding was provided by Institutional Support (LDRD) at Los Alamos and the DOE Office of Basic Energy Science (P.A.J.), by the National Science Foundation (C.M., H.S., M.K.), and by the United States Geological Survey (J.G.). We thank E. Brodsky, B. Behringer, N. Beeler and X. Jia for comments and reviews.

Author Contributions P.A.J., M.K., H.S. and C.M. designed the study. M.K., P.A.J. and C.M. designed and carried out the data collection procedure. P.A.J. and H.S. did most of the data analyses. P.A.J. and C.M. did most of the writing. P.A.J., H.S., M.K. and C.M. did the laboratory work and J.G. and C.M. did much of the writing interpretation. All authors contributed to the interpretation and writing.

Author Information Reprints and permissions information is available at www.nature.com/reprints. Correspondence and requests for materials should be addressed to P.A.J. (paj@lanl.gov).

METHODS

We use a double-direct shear configuration in a biaxial load frame, which applies a horizontal stress to three steel forcing blocks that contain symmetric layers of glass beads at the block interfaces (Fig. 1). A vertical piston drives the central block downward at a constant displacement rate to create shear. The apparatus is servo-controlled so that constant horizontal load and vertical displacement rate are maintained to ± 0.1 kN and $\pm 0.1 \mu\text{m s}^{-1}$, respectively. The applied stresses on the shearing layers are measured with strain-gauge load cells in series with each of the loading axes. The apparatus is controlled via computer, and recordings of the load, displacement and stresses are monitored throughout an experiment. The nominal frictional contact dimensions are $10 \text{ cm} \times 10 \text{ cm}$, the vertical displacement of the central block is $5 \mu\text{m s}^{-1}$, corresponding to a strain rate of approximately $1.2 \times 10^{-3} \text{ s}^{-1}$, and the horizontal stress is 4 MPa. The blocks are composed of 17-4 stainless steel with serrated faces of 1 mm wavelength and 0.75 mm depth, adjacent to the glass bead packs. The beads are class IV spheres and range in dimension from 105–149 μm , meaning the layers are each about 30 beads wide. The sample assembly is sheathed by a latex sleeve. In the experiments, horizontal loads of 1–15 MPa are explored as well. Background noise emanating from the building and instrument is well under 5×10^{-7} strain and at much lower frequency ($< \sim 100$ Hz) than the applied acoustic perturbations.

Vibration is applied via an acoustic source (Fig. 1): a Matec M50-2, 50-KHz central-frequency piezoceramic attached mechanically with clamps to the central block using vacuum grease as couplant and driven by a Samson 150, 75-watt amplifier. The signal is detected on the opposite face of the central block using a Brüel and Kjaer model 4393 accelerometer attached with beeswax, amplified by a Brüel and Kjaer 2635 charge amplifier, and recorded on computer. Acoustic frequencies range from 1–20 kHz. Such high frequencies are not part of the seismic spectrum in nature, which extends to 10–100 Hz at maximum, but are used to provide laboratory-scale physical insight that can be applied in nature. No frequency effect is observed in the observations presented. We initiate waves at a shear stress equal to $\sim 95\%$ of the failure strength by first measuring the stick–slip recurrence interval without wave excitation for approximately 30 events and then timing the initiation of vibration from the end of the previous stick–slip.

In the pulse experiments, a toneburst of 10–20 cycles with frequency ranging from 6.1–8.67 kHz is applied. We use tonebursts of approximately 3.3 ms duration and a centre frequency of 6,100 Hz for the results shown. In general, sound is applied every third stick–slip cycle after steady-state conditions are reached, but experiments were also conducted in which we applied sound at shorter and longer stick–slip intervals.

The strain amplitudes we apply range from about 5×10^{-7} to 8×10^{-6} . A strain wave of 10^{-6} applies a pressure of the order of 10^4 Pa, which is of the order of 1% of the normal stress. Elastic wave strain is estimated as follows. In a harmonic wave, strain $\varepsilon = du/dx$ is related to acceleration $\ddot{u} = d^2u/dx^2$

$$\varepsilon = \frac{\ddot{u}}{\omega c} = \frac{\dot{u}}{c} \quad (1)$$

for the time-average amplitude. We digitize the acceleration data and record the absolute value of the sinusoidal waveform with a sampling rate of 10 kHz at 16 bits.

Figure S1

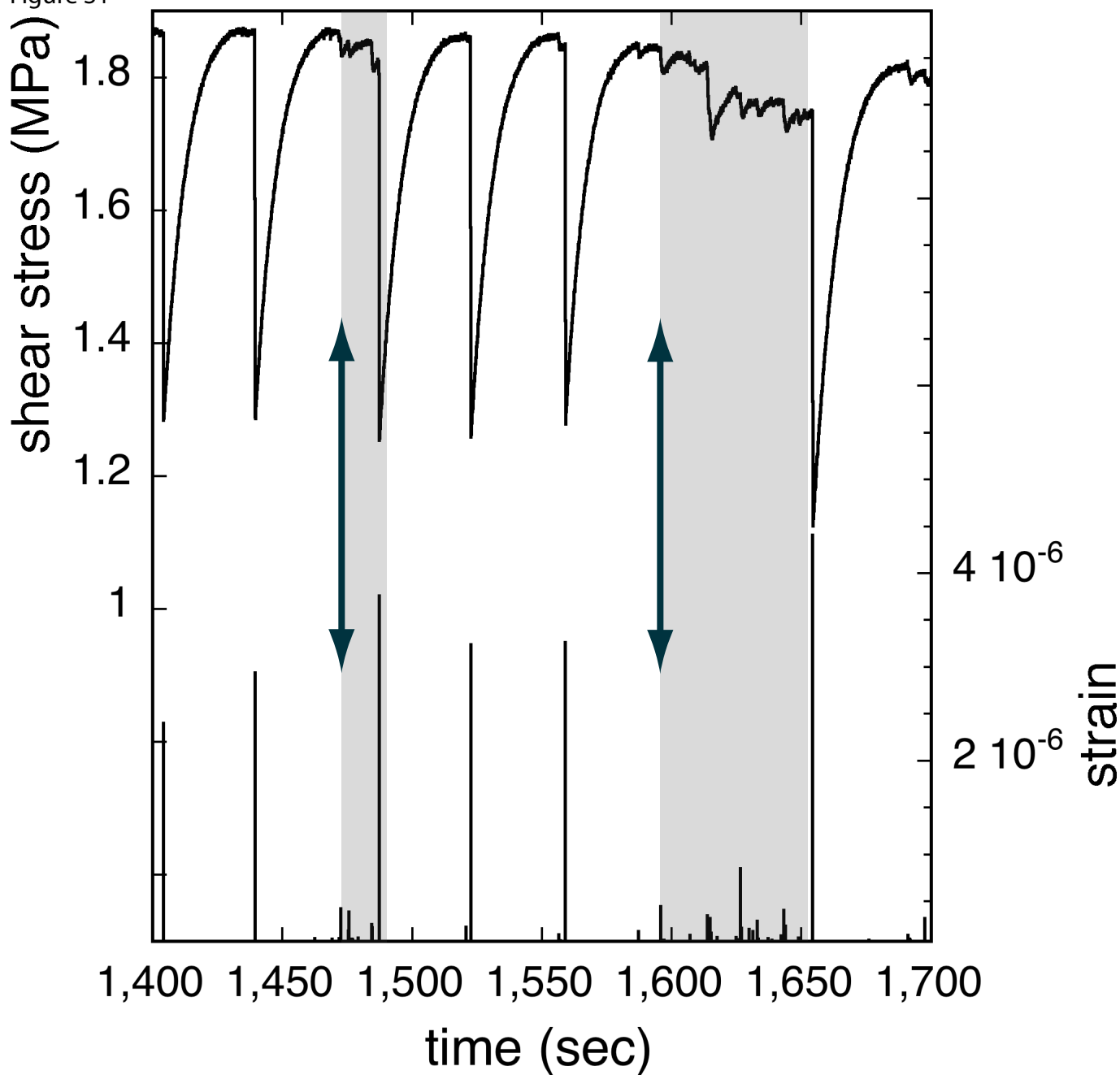


Figure S1: Example of pulse-mode dynamic straining. (top) Shear stress versus experimental time. (bottom) Measured, rectified strain amplitudes of the detected acoustic waves. Vertical arrows indicate acoustic pulse excitation times. Immediate and delayed triggering events are overlain in gray. A pulse was applied at ~ 1470 sec, and this in turn triggers a cascade of small stick-slip failures with accompanying acoustic emissions (e.g., $\sim 1470 - 1483$ sec). A consequence appears to be a delayed, major stick-slip event at ~ 1485 sec. The next acoustic pulse is applied at ~ 1595 sec, triggering a cascade of small events with acoustic emission (eg, $\sim 1605 - 1650$ sec), again leading to a delayed major event at ~ 1655 sec. p1087 refers to experiment number.

Figure S2

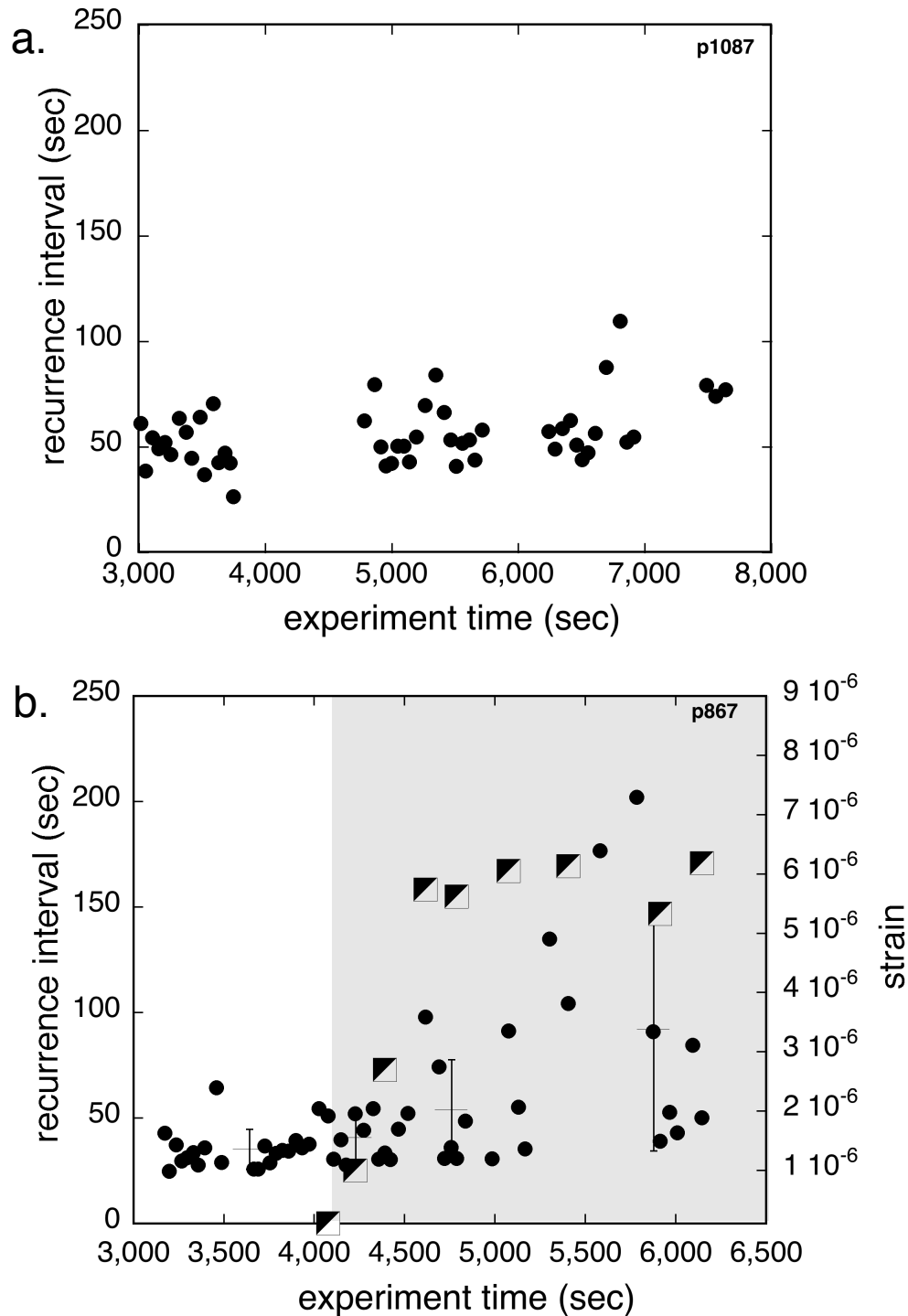


Figure S2: Experiments conducted at fixed versus increasing strain amplitude. (a) Recurrence in an experiment conducted at fixed dynamic strain of about 2×10^{-6} . Note that recurrence interval remains approximately the same (about 50 sec). (b) Results obtained where strain amplitude of the acoustic wave is progressively increased (half squares), overlain in light gray to show region of wave excitation (the first excitation was conducted at just over 4000 sec). The recurrence times are shown as solid circles. The mean recurrence time (horizontal lines) and standard deviation are noted. The increase in dynamic strain produces an increase in the mean recurrence as well as increased scatter (as indicated by the ± 1 standard deviation), in contrast to the constant amplitude experiment shown in (a). We have observed that, at dynamic strain amplitudes of less than about 10^{-6} no effect is induced for these loading and shearing conditions. More experiments aimed at addressing amplitude dependence of recurrence and memory are planned. p1087 and p867 refer to experiment numbers.